Korean J. Chem. Eng., **30**(4), 949-954 (2013)
DOI: 10.1007/s11814-013-0029-4

Synthesis and characterization of CdSe nanocrystals in the presence of butylamine as a capping agent

Nguyen Tam Nguyen Truong, Woo Kyoung Kim, and Chinho Park†

School of Chemical Engineering, Yeungnam University, 214-1 Dae-dong, Gyeongsan 712-749, Korea
(*Received 23 October 2012 • accepted 24 February 2013*)

Abstract−TOPO-capped cadmium selenide (CdSe) nanocrystals of sizes between 3 and 8 nm have been synthesized, and the surface-capping molecule, trioctylphosphine oxide, was replaced by butylamine. The effects of changing the surface ligands of the synthesized CdSe nanocrystals on the structural, optical, and electrical properties were investigated. The shift toward shorter wavelength (higher energy) in the visible range of the optical absorption band edge was observed by UV-Vis spectroscopy, and a blue-shift of the photoluminescence peaks was observed with luminescent quenching. Surface modification was found to cause an increase in the surface energy of nanocrystals, resulting in the improvement in charge carrier separation and cell performance in applications towards bulk hetero-junction solar cells.

Key words: Ligand Exchange, Nanocrystal, Blue-shift, Band Edge, Photoluminescence Quenching

INTRODUCTION

Colloidal semiconducting nanocrystals (NCs) are ubiquitous; nonetheless, they have been of scientific and nanotechnological interest [1,2]. In the past, they have been prepared in several sizes, ranging from nanometers to several micrometers. Colloidal nanocrystals have been widely used as building blocks for creating nano-assemblies, which are slated to be the next-generation nanodevices. Inorganic nanoparticles have attracted much attention in the last decade for their wide use in diverse research and industrial applications, including lasers, light-emitting diodes [3] and solar cells [4]. Nanometer-sized particles exhibit structural and optoelectronic properties that can be tuned by varying the size, shape, and surface-ligand of the particles, making them good candidates for blending with organic polymers within nano-devices [5].

CdSe nanocrystal possesses a band gap (E_g=1.74 eV) that lies in the visible spectrum and thus has been considered as an n-type partner in simple, low-cost, high performance bulk hetero-junction (BHJ) solar cells [6,7]. The BHJ solar cells using blends of conjugated polymer and inorganic nanocrystals were first reported in 1996 by Greenham, et al. [5] who showed that the addiction of CdSe NCs to polymers in solar cells relied on the ability of NCs to disperse within the polymer to create large interfacial surface area for electron/hole transfer between the two materials and to provide continuous pathways to the electrodes contact.

The BHJ solar cells utilizing the blend of CdSe nanocrystals and regioregular poly(3-hexylthiophene) (P3HT) polymer as a light absorption active layer have demonstrated power conversion efficiency of over 3%. Tetrapod-shaped CdSe nanocrystals are used in the world record CdSe BHJ solar cells, which indicated that the control of the nanocrystals shape and surface ligand in relationship with charge separation and dispersion characteristics is very important in improving the cell efficiency [8].

†To whom correspondence should be addressed.
E-mail: chpark@ynu.ac.kr

Synthesis and property characterization of CdSe nanocrystals have been widely studied by many research groups [6,7]. The effects of thermal annealing on the structural and optical properties of the CdSe nanocrystals have been recently reported by our group [9], indicating that after annealing in air- or N_2-atmosphere at 250 and 350 °C, the crystallinity and surface passivation characteristics of the CdSe nanocrystals are enhanced. Annealing-induced phase transitions were also observed, revealing that a significant change in the electrical and optical properties of nanocrystals could occur upon annealing. Sharma et al. reported the results of a quantitative study on the CdSe nanocrystals in the context of the effects of particle size and surface ligands on the photo-degradation of nanocrystals [10]. They concluded that the emission properties and lifetime of the CdSe nanocrystals are dependent upon the oxidation potential of the surface ligand and crystallite size. The influence of the atomic ratios of cadmium (Cd) to selenium (Se) in the CdSe nanoparticles upon optical and photoluminescence properties was also investigated [11]. It was shown that the shift of the optical absorption edge, concurrent with CdSe nanoparticle size reduction, agreed well with the quantum confinement effect. The effect of ligand choice on the hybrid solar cells has been investigated by many research groups [12-14]. The ligands having long carbon chains (e.g. trioctylphosphine oxide, TOPO) are typically involved in the synthesis of NCs as surfactants to control the size and shape of NCs, but these ligands can act as traps for charge carriers or can dominate the nanoparticles' electrical properties and work as insulating materials that reduce the charge transport [15], if they are not properly removed during the post-treatment (annealing). Thus other ligands such as pyridine, tributylamine (TBA) and butylamine (BA) are investigated as alternatives, since they have lower boiling points and higher electron affinities. However, the roles of the various different surface ligands of the nanocrystals, upon modifying the surface energy, optical, structural and electrical properties of the nanocrystals, remain mostly unexplored.

In this work, we studied the effects of surface ligand exchange and post nanocrystal synthesis upon the material properties of CdSe

nanocrystals. The chemical, structural and optoelectronic properties of the CdSe nanocrystals, before and after the exchange of the surfactants, were characterized systematically, and the related mechanisms were investigated.

EXPERIMENTAL

1. Chemical Preparation

All the chemicals used in this study are commercially available. Cadmium oxide (CdO) was purchased from Junsei Chem. Co., and solvents such as chloroform, chlorobenzene, and hexane were purchased from Duksan Chemical Co. Hexylphosphonic acid (HPA) was obtained from Alfa Aesar Chemicals, and selenium (Se) powder, trioctylphosphine (TOP), butylamine (BA), trioctylphosphine oxide (TOPO), and polyethylene dioxythiophene doped with polystyrene-sulfonic acid (PEDOT : PSS) were provided by Aldrich. Regioregular poly(3-hexylthiophene) (P3HT) polymer was supplied by American Dye Source, Inc. All reagents were used as-received without further purification.

2. Synthesis of CdSe Nanocrystals

The CdSe nanocrystals were synthesized by using a slightly modified hot injection method [16]. A stock solution of selenium powder (0.237 g) in TOP (5.0 mL) was stirred for over 24 h under a nitrogen environment in a glove box. Concurrently, 0.514 g of CdO, 3.7768 g of TOPO, and 0.2232 g of HPA were loaded into a two-neck flask. At approximately 320 °C, a colorless homogeneous solution was produced. The temperature was lowered to 250 °C, and the stock solution was rapidly injected into the two-neck flask. The nannoparticles were grown at 250 °C for 25 h to yield TOPO-capped CdSe.

2-1. Butylamine Treatment of TOPO-capped CdSe Nanocrystals

For ligand modifications, the TOPO-capped CdSe nanocrystals were dissolved in butylamine solvent, and the nanoparticles/butylamine mixture was stirred for 24 h at room temperature. Excess hexane was added to the solution to precipitate the CdSe nanoparticles. The precipitated nanoparticles were then centrifuged three times to yield high-purity butylamine-capped CdSe nanocrystals. Finally, the BA-capped CdSe nanocrystals were dried in an oven under vacuum at 60 °C.

2-2. Characterization of CdSe Nanocrystals

UV-Vis spectra were measured in hexane or chlorobenzene on a Cary 500, using 1.0-cm path length quartz cells. The size and shape of the nanocrystals were estimated with a high-resolution transmission electron microscope (HR-TEM, H-7600). The nanocrystal structure was measured by powder X-ray diffraction (XRD) on an MPD PANalytical, using CuKα radiation. The optical properties and chemical composition of CdSe nanocrystals were measured by photoluminescence (PL) spectroscopy and X-ray photoelectron spectroscopy (XPS). Fourier transform infra-red (FT-IR) spectra were recorded in the range of 450-4,000 cm^{-1}, using the Excalibur Series FTS 3000 spectrometer (BioRad) at a resolution of 16, with 32 scans in a form of KBr pellet.

2-3. Bulk Hetero-junction Solar Cell Fabrication

The procedure to prepare the blend of CdSe and P3HT was as follows: A solution of the TOPO- or BA- capped CdSe nanoparticles was blended with P3HT, which was dissolved in the binary solvent of chlorobenzene and pyridine mixture. In all cases, the weight ratio of the CdSe/P3HT was kept at 7 : 3, while the volumetric ratio of chlorobenzene/pyridine was kept at 8 : 2.

BHJ solar cells were prepared by the bulk hetero-junction layer of the CdSe/P3HT being spun on top of a cleaned indium tin oxide (ITO)-coated glass, serving as the anode, which was covered with PEDOT : PSS as a hole transport layer (HTL), and an Al layer as the cathode. In detail, the ITO substrate was cleaned with trichloroethylene (TCE), acetone, and methanol (10 min each) in a wet station. The cleaned ITO-coated glass was then plasma-treated under N_2 for 10 min. The HTL, PEDOT : PSS was spin-coated onto the cleaned substrate and then dried at 100 °C for 30 min. The active layer, CdSe/P3HT blend solution was spin-coated on top of the PEDOT : PSS layer, then dried at 140 °C for 30 min. Finally, serving as the cathode, the devices were completed by thermal evaporation of aluminum (100 nm) on the top of the device structure. Before J-V measurement, the completed devices were annealed at 140 °C for 10 min on a hot plate under nitrogen environment in an N_2 glove box. The current density-voltage (J-V) characteristics of the fabricated cells were investigated under AM 1.5G illumination, using a solar simulator (Keithley 69911).

RESULTS AND DISCUSSION

The FT-IR spectra of the TOPO-capped CdSe nanocrystals and BA-capped CdSe nanocrystals are presented in Fig. 1. In Fig. 1(a), the P=O stretching vibration mode from TOPO molecules on the CdSe nanocrystal surface was observed at 1,088 cm^{-1} which is in good agreement with the literature reported value [17,18]. The bands near 2,854 and 2,924 cm^{-1} can be assigned to the C-C-H stretching vibration of the TOPO ligands [17]. In Fig. 1(b), however, the peaks at 1,088, 2,854 and 2,924 cm^{-1} of the TOPO ligands are nearly absent, implying that the TOPO surfactants were removed under the detection limit by the ligand exchange process. Presence of butylamine is indicated by the presence of the peaks at ~3,700-3,780 cm^{-1} corresponding to the N-H stretching vibration modes from butylamine molecules [19].

Fig. 2 shows the UV-Vis and PL spectra of the CdSe nanocrystals capped with TOPO and BA ligands, respectively. CdSe nanoc-

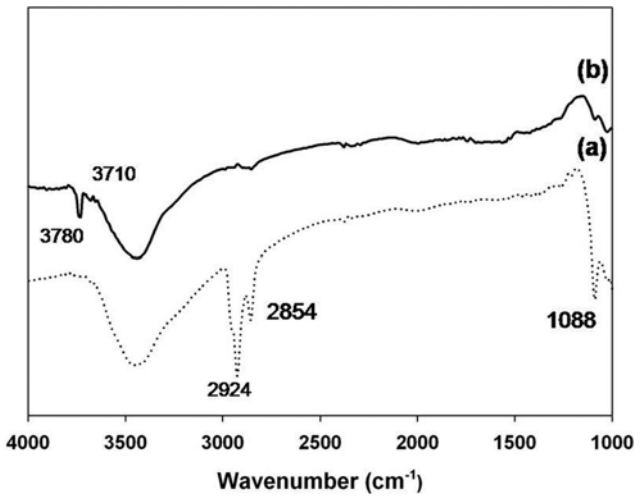

Fig. 1. FT-IR spectra of CdSe nanocrystals: (a) TOPO-capped CdSe and (b) butylamine-capped CdSe nanocrystals.

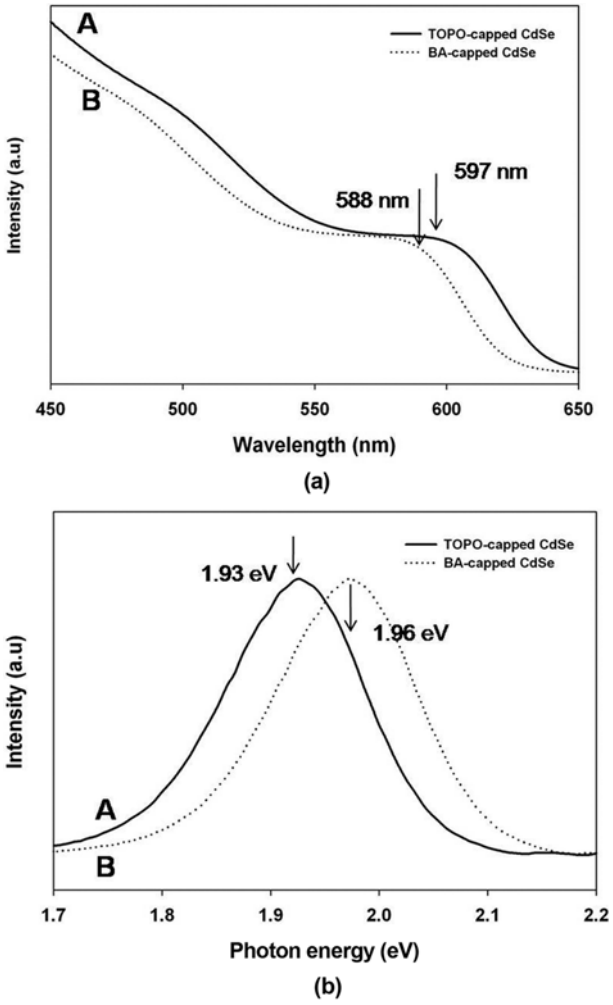

Fig. 2. UV-vis absorption (a) and photoluminescence (b) spectra of CdSe nanocrystals: (A) capped with TOPO and (B) capped with butylamine ligands.

rystals were dispersed in chlorobenzene prior to the spectroscopy measurements. After the ligand exchange from TOPO to butylamine, the absorption edge of the UV-Vis spectra was shifted to a shorter wavelength from 597 to 588 nm as shown in Fig. 2(a), and the emission peak of the PL spectra shifted towards a higher energy from 1.93 to 1.96 eV as shown in Fig. 2(b). The shifting of the absorption edge and emission peak toward a shorter wavelength is often referred to as a blue-shift; this could be due to the quantum confinement effect on account of reduction in nanocrystal size [20,21]. Surface defects related to the emission property change could also be generated in nanocrystalline semiconducting materials. Since the smaller-sized nanocrystals possess a larger surface-to-volume ratio compared to the larger-sized nanocrystals, and most of the photogenerated charge carriers undergo recombination at the surface vacancies, the luminescence of smaller nanocrystals is likely much stronger. However, the quenching of PL intensity was observed in this study from the nanocrystals after the ligand exchange from TOPO to butylamine, contradicting the literature report [20].

The size and structural properties of the CdSe nanocrystals were measured by HR-TEM, as shown in Fig. 3. The lattice fringes were clearly observed from HR-TEM images of both TOPO- and BA-capped CdSe nanocrystals as shown in Fig. 3(b) and 3(d), indicating that the nanocrystals are highly crystalline in a cubic structure [22,23]. From the measurement of the size of CdSe nanocrystals in TEM images as displayed in Fig. 3(a) and 3(c), the nanocrystal sizes were found to be ~3-8 nm for both TOPO- and BA-capped nanocrystals. The average size of the CdSe nanocrystals was calculated from the particle size distribution histograms. The size of the individual CdSe nanoparticle was first measured manually from 100 particles in each TEM micrograph, and then the average particle size was calculated by using the following equation:

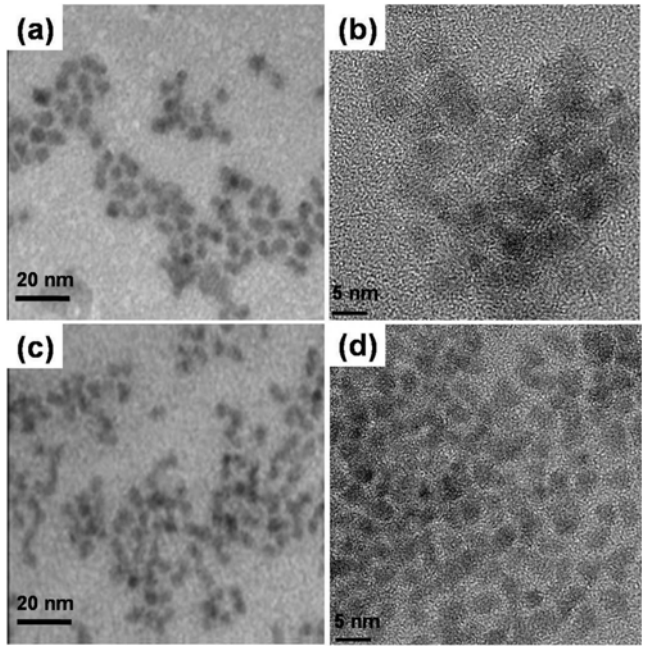

Fig. 3. TEM and HR-TEM images of CdSe nanocrystals capped with (a), (b) TOPO and (c), (d) butylamine.

$$S = \frac{\Sigma_{i=0}^{N} S_i}{N} \quad (1)$$

where S_i is the size of the particle i, and N is the total number of particles (in this study N=100).

The particle size distribution histogram of TOPO-capped CdSe is shown in Fig. 4(a), which indicates the fraction of the particles with a diameter in the range of 3-8 nm. The average particle size of the TOPO-capped CdSe was 5.68 nm, calculated using Eq. (1). Fig. 4(b) shows the particle size distribution of BA-capped CdSe with the average particle size of 4.66 nm. The average particle size of the BA-capped CdSe was reduced by 1.02 nm from that of the TOPO-capped CdSe. As expected from the optical measurement results, the reduction in nanocrystal size during the ligand exchange procedure was confirmed by the TEM micrographs. The decrease in nanocrystal size during the ligand exchange process is explained by the possible loss of Cd and Se atoms present on the nanoparticle surface [24] which makes the nanocrystals shrink in size. Removal of surface atoms was facilitated by the relatively high defect density on the surface, as well as the high surface energy. The reduction in nanocrystal size subsequently caused the blue-shifts in the absorption edge and the photoluminescence peaks. It is further speculated that the PL quenching observed from the samples presented

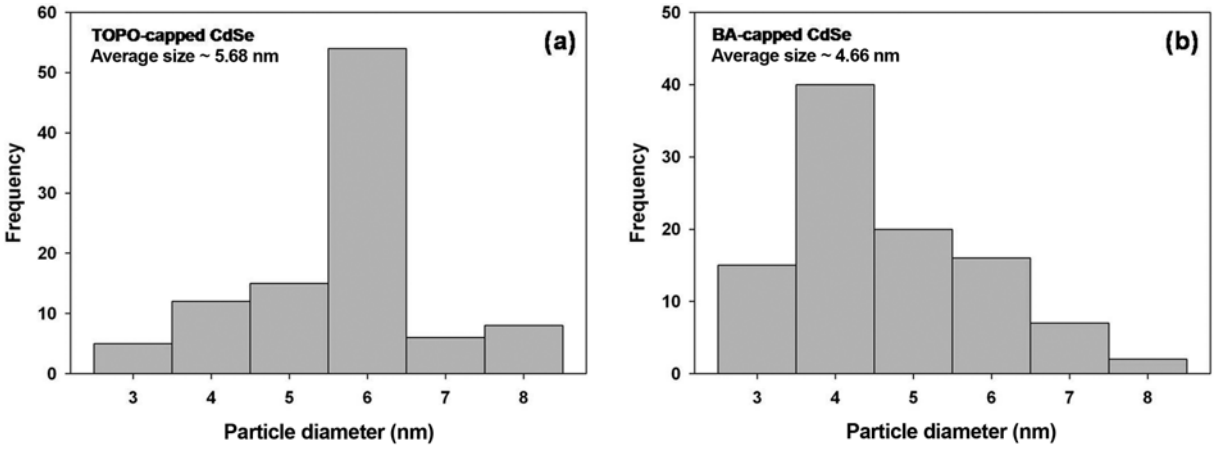

Fig. 4. Size distribution histograms of CdSe nanocrystals: (a) TOPO-capped and (b) butylamine-capped CdSe nanoparticles.

within this study indicates the removal of surface defects and subsequent passivation of the surface by the electron-donating amine ligands.

XRD scans of the CdSe nanoparticles (TOPO- and BA-capped) were performed in order to determine the crystal structure. In Fig. 5(a), pattern (A) shows the XRD of TOPO-capped CdSe samples, exhibiting three diffraction peaks at 2θ=25.3°, 42.01°, and 49.52°, corresponding to the (111), (220), and (311) planes of reflection for the cubic phase of the bulk CdSe nanoparticles from the JCPDS (Joint Committee for Power Diffraction Set) database No. 19-0191.

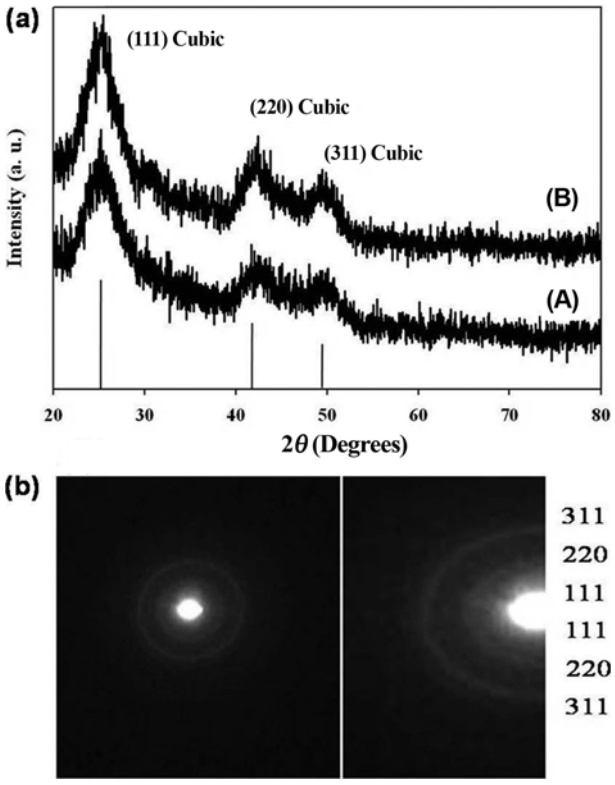

Fig. 5. (a) X-ray diffraction patterns of CdSe nanocrystals with (A) TOPO-capped, (B) butylamine-capped; (b) selected area electron diffraction (SAED) patterns of TOPO-capped CdSe nanocrystals.

Pattern (B) in Fig. 5(a) shows the XRD of the BA-capped CdSe samples, showing three diffraction peaks at 2θ=25.80°, 42.28°, and 49.86°, which can be assigned also to the (111), (220), and (311) planes of reflection of the cubic phase. It was observed that the (111), (220), and (311) peaks of BA-capped CdSe were slightly shifted towards higher scattering angles compared those of TOPO-capped CdSe, indicating that nanocrystal size was decreased. The XRD results again match well with the TEM results. The structure of nanoparticles was further confirmed by selected area electron diffraction (SAED). Fig. 5(b) shows the SAED pattern of the TOPO-capped CdSe samples, revealing the (111), (220), and (311) planes of the cubic phase of CdSe [22,23], which is again in good agreement of the XRD results. From the above results, we concluded that the crystal structure remains unchanged (cubic phase) by the ligand exchange procedure.

The effects of the ligand exchange upon the chemical bonding characteristics of the CdSe nanocrystals were investigated by X-ray photoelectron spectroscopy (XPS). Fig. 6 shows the XPS survey spectra of the TOPO- and BA-capped nanocrystals. The general survey spectrum mainly reveals the Cd and Se peaks from the nanocrystals, even though the C and O peaks were also observed,

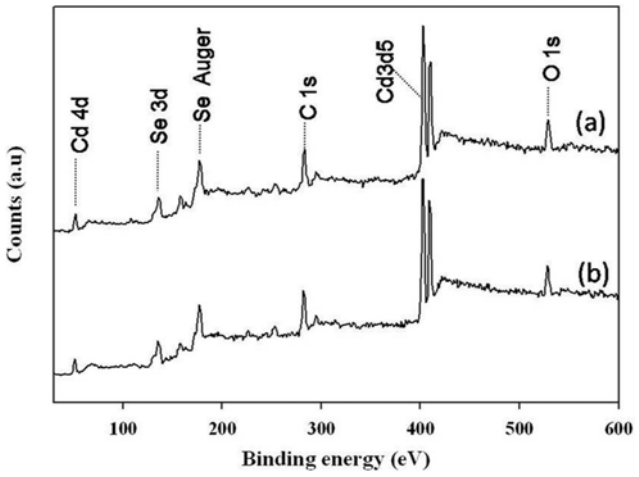

Fig. 6. XPS survey spectra of CdSe nanocrystals: (a) TOPO-capped CdSe, (b) butylamine-capped CdSe nanocrystals.

indicating the presence of surface ligands. The survey spectra obtained from CdSe nanocrystals with different surface ligands were identical to each other in terms of the number of peaks and their positions, which were also close to the bulk values [25]. High-resolution XPS spectra were obtained for the samples of the TOPO- and BA-capped CdSe; the corresponding Cd 3d, Se 3d, and O 1s peaks are shown in Fig. 7(i-iii), respectively. As shown in Fig. 7(i)-(a), the presence of the Cd $3d_{5/2}$ peak at 402.34 eV indicated that the Cd exists either in a metallic (unreacted Cd) or CdSe form [26]. Fig. 7(i)-(b) shows the Cd $3d_{5/2}$ peak at 404.2 eV indicating the shift of 1.86 eV toward a higher binding energy state after the ligands were changed from TOPO to BA. The decrease in the intensity of the Cd 3d levels was believed to be caused not by surface oxidation, but by formation of stronger bonding within the CdSe nanocrystals. Fig. 7(ii) shows the XPS spectra for the Se 3d. In the case of TOPO-capped CdSe nanocrystals (curve A), the Se 3d peak position was observed at 50.92 eV, while it was observed at 52.82 eV for the BA-capped samples, shifting 1.89 eV toward the higher binding energy state. The presence of Se 3d at 50.92 and 52.82 eV, and the lack of peaks near 60 eV, further confirms the CdSe-only phase (absence of Se oxides) [27,28]. Fig. 7(iii) shows the XPS spectra from the O 1s region; the O 1s peak was observed at 528.16 eV for TOPO-capped nanocrystals (curve A), whereas for BA-capped CdSe samples (curve B), the O 1s peak was shifted toward a higher binding energy (by 2.27 eV). The presence of C 1s at ~282 eV was also identified [29]. The XPS studies also confirmed the absence of cadmium oxide, hydroxide, and selenium oxide, indicating that high-purity CdSe nanocrystals were synthesized in this study.

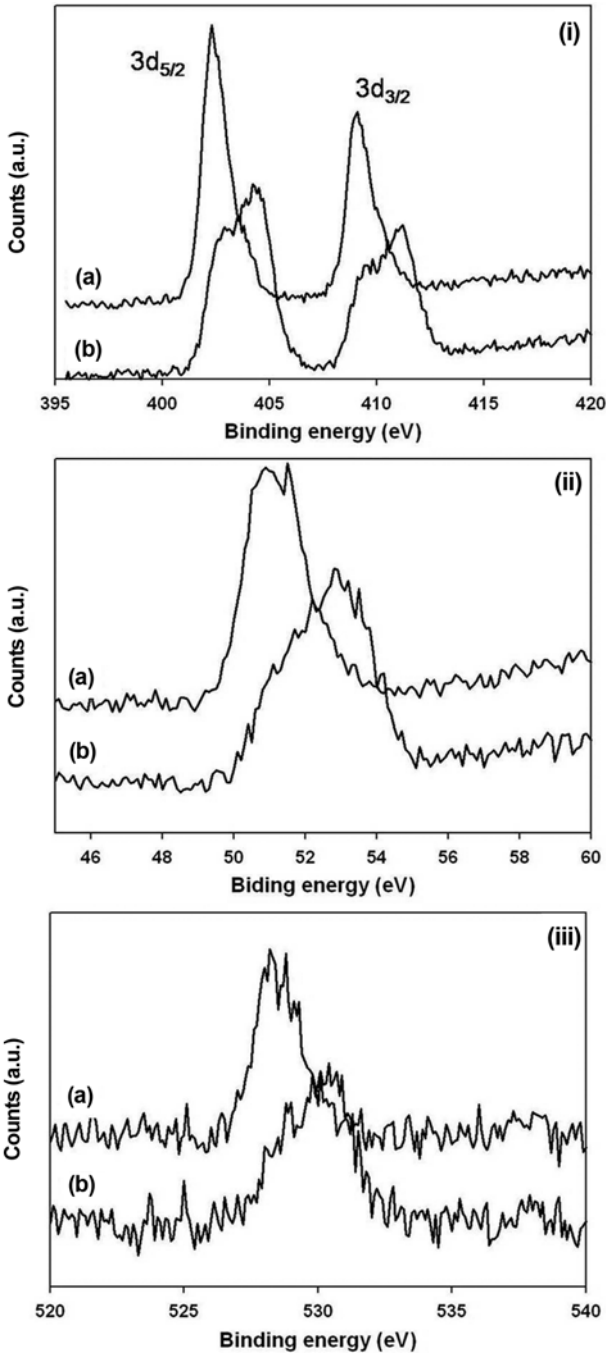

Fig. 7. XPS spectra of CdSe nanocrystals with (a) TOPO-capped and (b) butylamine-capped: (i) XPS spectra corresponding to the Cd 3d region; (ii) XPS spectra corresponding to the Se 3d region; (iii) XPS spectra corresponding to the O 1s region.

To study the impact of ligand exchange upon suitability for application of CdSe nanocrystals in photovoltaic devices, different ligand-capped CdSe nanoparticles were used in BHJ solar cells. The BHJ solar cells of the structure, ITO-coated glass (ITO thickness of 180 nm)/PEDOT : PSS (70 nm)/(CdSe+P3HT) (150 nm)/Al (100 nm), were fabricated by using a blend of P3HT as the electron-donor material and CdSe nanoparticles as the electron-acceptor material (both TOPO- and BA-capped CdSe) in the binary solvents of chlorobenzene/pyridine. The power conversion efficiency of the fabricated devices was measured under AM1.5 illumination, in an N_2 glove box at room temperature. The power conversion efficiency of the cells made of TOPO-capped CdSe nanoparticles turned out to be ~0.55%; however, cells made of BA-capped CdSe nanoparticles under identical conditions showed an efficiency of around 1%. The high-quality nanoparticles improved the BHJ solar cell performance. Interestingly, it was observed in the J-V curves of the cells (shown in Fig. 8) that there was an increase in the short circuit current (J_{sc} from 1.42 to 2.69 (mA/cm^2), when the ligand was changed

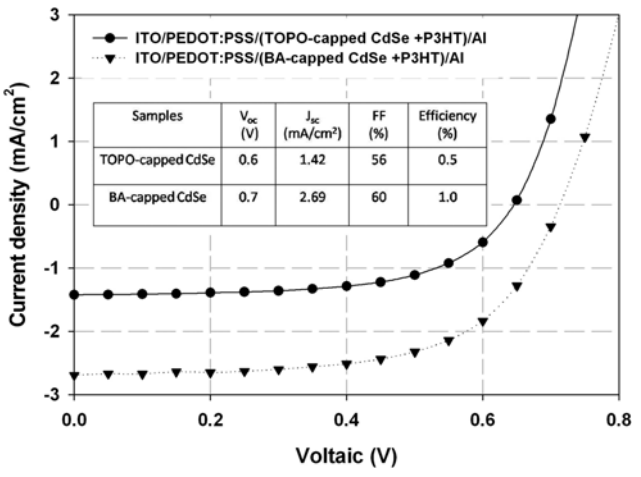

Fig. 8. I-V curves of the solar cells made with TOPO- and butylamine-capped CdSe nanoparticles (CdSe/[CdSe+P_3HT]= 0.7).

from TOPO to BA, while the open circuit voltage (V_{oc}) remained almost the same. The power conversion efficiency of BHJ solar cells fabricated in this study is, however, still relatively low compared with that of world record BHJ solar cells made with tetrapod-shaped CdSe nanocrystals and P3HT polymers, possibly attributable to the poorer charge collection due to nanocrystals' shape, and poorer interfacial integrity between the polymer and CdSe nanoparticles, creating a phase separation within the active surface morphology.

In review of the literature, similar power conversion efficiencies of approximately 0.05% [30] were achieved with spherical CdSe nanoparticles and a P3HT active layer of BHJ solar cells. The CdSe nanoparticle ligands were modified from TOPO- to pyridine-capped by a liquid-liquid exchange process. In this study, the CdSe (of spherical shape) nanoparticle ligands were modified from TOPO- to BA-capped, achieving a better power conversion efficiency with the BA-capped CdSe. These values were slightly smaller than those previously reported with a blend of nanorod-CdSe and P3HT, of which efficiencies can approach ~1% with optimization of the active layer morphology, mixing ratio, thermal annealing, multiple ligand exchange, and film thickness [31,32]. We thus conclude that the efficiencies obtained from this study open a new route to improving bulk hetero-junction solar cells by considering another type of ligand for the CdSe nanoparticles. The ligand exchange process could also be applied to differently shaped CdSe nanocrystals such as tetrapod-shaped and hyperbranched nanocrystals for further improvement in the power conversion efficiency.

CONCLUSIONS

Highly crystalline, pure and cubic CdSe nanocrystals of spherical shape were successfully synthesized in this study, and the influence of exchanging the surface ligands on the synthesized CdSe nanocrystals upon structural, optical, and electrical properties was characterized in detail. After the ligand exchange, the nanocrystals' size was slightly reduced, resulting in higher surface energy, subsequently causing a blue-shift in the UV-vis absorption edge and photoluminescence peaks. Photoluminescence quenching was also observed due to the removal of surface defects and enhancement of surface passivation during the ligand exchange. Improvement in charge carrier separation at the nanoparticle-polymer interface was expected to occur, resulting in the increased short circuit current.

ACKNOWLEDGEMENTS

This research was supported by the Basic Science Research Program through the National Research Foundation of Korea (NRF) funded by the Ministry of Education, Science and Technology (2010-0023839), and the Human Resources Development Program of Korea Institute of Energy Technology Evaluation and Planning (KETEP) grant (No. 20104010100580) funded by the Korean Ministry of Knowledge Economy.

REFERENCES

1. D. J. Suh, O. O. Park, H. T. Jung and M. H. Kwon, *Korean J. Chem. Eng.*, **19**, 529 (2002).
2. Y. B. Hahn, *Korean J. Chem. Eng.*, **28**, 1797 (2011).
3. M. Artemyev, U. Woggon and W. Langbein, *Physica Status Solidi*, **229**, 423 (2002).
4. N. Amin, K. Sopian, M. Yahya and A. Zaharim, *8th WSEAS. International Conference on Power Systems*, **23** (2008).
5. N. C. Greenham, X. G. Peng and A. P. Alivisatos, *Physical Review*, **54**, 17628 (1996).
6. W. U. Huynh, J. J. Dittmer, W. C. Libby, G. L. Whiting and A. P. Alivisatos, *Adv. Funct. Mater.*, **13**, 73 (2003).
7. I. E. Anderson, A. J. Breeze, J. D. Olson, L. Yang, Y. Sohoo and S. A. Carter, *Appl. Phys. Lett.*, **94**, 063101 (2009).
8. S. Dayal, M. O. Reese, A. J. Fergusion, D.S. Ginley, G. Rumbles and N. Kopidakis, *Adv. Funct. Mater.*, **20**, 2629 (2010).
9. U. Farva and C. Park, *Sol. Energy Mater. Sol. Cells*, **94**, 303 (2010).
10. S. N. Sharma, H. Sharma, G. Singh and S. M. Shivaprasad, *Mater. Chem. Phys.*, **110**, 471 (2008).
11. S. N. Sharma, H. Sharma, G. Singh and S. M. Shivaprasad, *Physica E.*, **31**, 180 (2006).
12. J. D. Olson, G. P. Gray and S. A. Carter, *Sol. Energy Mater. Sol. Cells*, **93**, 519 (2009).
13. K. M. Noone, N. C. Anderson, N. E. Horwitz, A. M. Munro, A. P. Kulkarni and D. S. Ginger, *ACS Nano.*, **3**, 1345 (2009).
14. P. Reiss, E. Couderc, J. De Girolamo and A. Pron, *Nanoscale*, **3**, 446 (2011).
15. G. Kalyuzhny and R. W. Murray, *J. Phys. Chem. B*, **109**, 7012 (2005).
16. Z. A. Peng and X. Peng, *J. American Chem. Soc.*, **123,** 183 (2001).
17. I. S. Liu, H. H. Lo, C. T. Chien, Y. Y. Lin, C. W. Chen, Y. F. Chen, W. F. Su and S. C. Liou, *J. Mater. Chem.*, **18**, 675 (2008).
18. B. J. Landi, C. M. Evans, J. J. Worman, S. L. Castro, S. G. Baily and R.P. Raffaelle, *Mater. Lett.*, **60**, 3502 (2006).
19. G. Ramis, *J. Molecular Structure*, **193**, 93 (1989).
20. N. Chandrasekharan and P. V. Kamat, *Research on Chemical Intermediates*, **28**, 847 (2002).
21. J. H. Adair, T. Li, T. Kido, K. Havey, J. Moon, L. Mecholsky, A. Morrone, D. R. Talham, M. H. Lugwig and L. Wang, *Mater. Sci. Eng. R.*, **23**, 139 (1998).
22. J. E. Bowen Katari, V. L. Colvin and A. P. Alivistos, *J. Phys. Chem.*, **98**, 4109 (1994).
23. S. Chen. X. Zhang, Y. Zhao, J. Yan and W. Tan, *Mater. Lett.*, **63**, 712 (2009).
24. C. Querner, P. Reiss, S. Sadki, M. Zagorska and A. Pron, *Phys. Chem. Chem. Phys.*, **7**, 3204 (2005).
25. C. J. Vesely and D. W. Langer, *Physical Review B*, **4**, 451 (1971).
26. M. Azad Malik, N. Revaprasadu and P. O'Brien, *Chem. Mater. Lett.*, **13**, 913 (2001).
27. D. P. Masson, D. J. Lockwood and M. J. Graham, *J. Appl. Phys.*, **82**, 1632 (1997).
28. Q. Yang, K. Tang, F. Wang, C. Wang and Y. Quian, *Mater. Lett.*, **57**, 3508 (2001).
29. C. D. Wangner, Handbook of X-ray Photoelectron Spectroscopy, Perkin-Elmer Corp., Eden Prairie 50 (1979).
30. S. H. Choi, H. Song, I. K. Park, J. H. Yum, S. S. Kim, S. Lee and Y. E. Sung, *J. Photochem. Photobiol. A: Chem.*, **179**, 135 (2006).
31. I. Lokteva, N. Radychev, F. Witt, H. Borchert, J. Parisi and J. K. Olesiak, *J. Phys. Chem.*, **114**, 12784 (2010).
32. P. E. Shaw, A. Ruseckas and I. D. Samuel, *Adv. Mater.*, **20**, 3516 (2008).